MASSACHUSETTS INSTITUTE OF TECHNOLOGY

LINCOLN LABORATORY

SPACE COMMUNICATIONS

QUARTERLY TECHNICAL SUMMARY REPORT TO THE AIR FORCE SYSTEMS COMMAND

1 MARCH – 31 MAY 1977

ISSUED 22 AUGUST 1977

LEXINGTON MASSACHUSETTS

The work reported in this document was performed at Lincoln Laboratory, a center for research operated by Massachusetts Institute of Technology, with the support of the Department of the Air Force under Contract F19628-76-C-0002.

This technical report has been reviewed and is approved for publication.

FOR THE COMMANDER

Raymond L. Loiselle

Raymond L. Loiselle, Lt. Col., USAF
Chief, ESD Lincoln Laboratory Project Office

INTRODUCTION

This Space Communications – Division 6 Quarterly Technical Summary covers the period 1 March through 31 May 1977. It includes satellite communications work performed within Divisions 6 and 7. Other work in Division 6 is reported separately.

LES-8/9 and the associated terminals continue to operate as before. Most of the Lincoln Laboratory communications experiments and demonstrations have now been completed. Tests with AFAL, Aerospace, MITRE, and Service contractors continue.

Activity is continuing with analysis, initial design, and the start of hardware for ground testing in the two major technology areas – adaptive antenna nulling and on-board satellite processing.

Barney Reiffen
Head, Communications Division

Charles W. Niessen
Associate Head

15 June 1977

CONTENTS

REPORTS ON SPACE COMMUNICATIONS

1 March through 31 May 1977

PUBLISHED REPORTS

Technical Note

TN No.				DDC No.
1977-14	A Survey of Solid-State Microwave Power Devices	P. W. Staecker D. F. Peterson	29 April 1977	AD-A041202

Meeting Speeches

MS No.			
4366	A Linear-Filtering Transform Algorithm Based on Permutations	C. M. Rader P. F. McKenzie	IEEE-ASSP Intl. Conf. Record, 9-11 May 1977, pp. 45-48
4403	Precision Oscillators Flown on the LES-8/9 Spacecraft	H. S. Babbitt	Proc. 31st Annual Symp. on Frequency Control, Atlantic City, 1-3 June 1977

Anechoic Chamber Study

			DDC No.
Final Report	RF Anechoic Chamber Study, Vol. 3: Architectural Design and Cost Estimate of RF Anechoic Chambers	1 April 1977	*

* Not yet assigned.

ORGANIZATION

DIVISION OFFICE

B. Reiffen, *Division Head*
C. W. Niessen, *Associate Head*
S. Gould, *Assistant*

R. M. Lerner
C. R. Peatfield

GROUP 61

L. J. Ricardi, *Leader*
A. J. Simmons, *Associate Leader*

Burns, R. J.
Burrows, M. L.
Cummings, W. C.
Dion, A. R.
Frediani, D. J., Jr.
Lee, J. C.
Lim, H. K.
Lindberg, C. A.
Mayhan, J. T.
Niro, L.
Potts, B. M.
Turbett, T. M.
Weikle, D. C.
Weiner, H.

GROUP 63

L. W. Bowles, *Leader*
R. S. Berg, *Associate Leader*

Babbitt, H. S.
Bauer, R. F.
Berglund, C. D.
Collins, C. J.
Dolbec, R. E.
Hodsdon, D. M.
Robbio, T. P.
Safran, M.
Small, C. E.
Solman, F. J., III
Staecker, P. W.
Stevens, M. L.

GROUP 64

T. S. Seay, *Leader*
W. W. Ward, *Associate Leader*
D. R. McElroy, Jr., *Assistant Leader*

Collins, L. D.
Curley, C. R.
Ewing, D.
Giordano, J. L.
Gjelsvik, A. M.
Hamilton, K. R.
Harvey, R. L.
Hoover, H. H., Jr.
Hutchinson, W. K.
Jones, L. R.
Liias, G. G.
MacPhee, J. V.
Pelletier, R. J.
Provencher, W. C.
Rafuse, R. P.
Sarantos, T.
Siegel, D. A.
Willim, D. K.

GROUP 66

S. L. Bernstein, *Leader*
R. W. Chick, *Associate Leader*

Capetanakis, J. I.*
Hazel, D. F.
Heggestad, H. M.
Helfrich, J. H.
Levasseur, A. H.
McNeill, D. A.
Perry, K. E.
Saklad, M. S.
Sellers, G. W.
Siemasko, J. F.
Storch, S. B.
Swanton, C. B.
Taylor, L. E.
White, D. P.
Zeuli, H. E.

GROUP 67

B. H. Hutchinson, *Associate Leader*

Bucher, E. A.
DeRosa, J. K.
Eaves, R. E.
Kalet, I.
Metzger, L. S.
O'Leary, G. C.
Weiner, L. N.
Wilson, R. A.

GROUP 68

F. W. Floyd, Jr., *Leader*
D. M. Snider, *Associate Leader*

Conrad, P. J., Jr.
Davis, E. S.
Flanders, G. T.
Hart, J. M.
Millner, A. R.
Petersen, W. A.
Sullivan, R. F.
Trudeau, N. R.
Vernau, J. R.
Vondra, R. J.
Walther, F. G.
Woods, J. P.
Wright, J. N.

GROUP 69

F. W. Sarles, Jr., *Leader*
C. M. Rader, *Assistant Leader*

Coomber, D. B.
Culmone, A. F.
Gagnon, G. P.
Godfrey, B. W.†
Hale, A. F.
Johnson, D. H., Jr.
MacInnes, R. D.
McKenzie, P. F.
Morton, S. G.
Rhodes, R. R.
Roberge, J.‡
Rogers, D. C.
Sitler, D. G.
Smith, W. B.
Srivastava, S.
Tai, C. H.
White, N. B.

---

* Research Assistant.

† Part time.

‡ Consultant.

CONTRIBUTORS
TO
SPACE COMMUNICATIONS PROGRAM

DIVISION 7

J. F. Hutzenlaub, *Division Head*
P. Waldron, *Associate Head*
A. E. Johnson, *Assistant*

GROUP 71

Blaisdell, E. W.	Greaves, A. W.	McLaughlin, J. D.
Boisclair, W. F.	Hagerman, A. H.	Murphy, E. B.
Bouvier, A. J.	Harney, W. F.	Purdy, R. W.
Brawn, M. W.	Heaslip, D.	Staffiere, A. R.
Caunt, J.	Hom, S.	Sullivan, C. M.
D'Arcangelo, A. J., Jr.	Knowles, P. G.	Wainwright, E. S.
Furnsworth, L. P.	Kutney, M.	Weidler, D. E.
Folino, F. A.	Leyenaar, A. R.	Young, R. W.
Gordon, L. J.	MacKay, R.	

GROUP 72

Howitt, A. J.	Pappas, C. A.	Thompson, D. W.
Milne, J., Jr.	Sanderson, A. M.	

GROUP 73

Britten, S. S.	MacDonald, H. A.	Stevens, E. J.
Grossman, B. L.	Nathanson, D. M.	

GROUP 76

Bagley, D. G.	Gillaspie, C. L.	Routenberg, W. A.
Connelly, J. J.	Letteney, F. K.	Ryan, J. L.
Fitzgerald, W. J.	Rich, A. M.	

ANTENNAS
GROUP 61

I. INTRODUCTION

Group 61 is concerned with the development of antennas and associated microwave components. Particular emphasis is placed on satellite, ground, and airborne antenna systems.

II. TECHNOLOGY PROGRAM

A. Introduction

As part of its satellite communications program, Lincoln Laboratory is studying a number of techniques which might permit more effective military satellite communications systems to be realized.

MILSATCOM systems should discriminate between desired signals and interference. Modulation techniques which spread the signal bandwidth beyond that required by the data rate are widely used for this purpose. Additional discrimination can be obtained in principle by designing a receiving antenna which discriminates adaptively between signal and interference on the basis of direction. We have begun to study the feasibility of such a spacecraft antenna system operating at UHF.

B. Scale-Model Measurements

The manually controlled weight network described in the previous Quarterly Technical Summary† was used with the 7-element feed and UHF quarter-scale paraboloid multibeam antenna to determine the nominal nulling bandwidth of the antenna system for various jammer scenarios. An eighth channel, making use of a weighted array, was added which offers the flexibility of using either the seven multiple beams as an earth-coverage reference (i.e., quiescent pattern) or the separate eighth-channel earth-coverage array as reference. The procedure used to set the weights to their quantized values was described in the previous Quarterly Technical Summary, and the achievable null depths are subject to the errors described therein. After setting the weights for a particular frequency, a plot of null depth vs frequency was measured over a particular band of interest about the nulling frequency. Particular bandwidths of interest are 1.5 percent (5-MHz bandwidth at 350 MHz) and 3 percent (10-MHz bandwidth at 350 MHz). Over these two bands, average null depths (relative to peak antenna gain) of −30 dB and −25 dB, respectively, were consistently obtained for various single-jammer scenarios.

As a consequence of these results, a more detailed study of the various factors affecting null depth is being undertaken. Simulations have indicated that a constraint on the quiescent radiation pattern has a significant effect on the achievable nulling bandwidth due to the frequency sensitivity of the canceling beam relative to the reference pattern. A new automated test system currently being installed at the Antenna Test Range (ATR) will enable more precise data to be obtained relative to the frequency response of each output port contributing to the nulled pattern. The test system is essentially checked out, and should be operational in the coming month.

---

† Space Communications – Division 6 Quarterly Technical Summary, Lincoln Laboratory, M.I.T. (15 March 1977), p. 1, DDC AD-B019468-L.

The test system is currently being programmed to automate the process of collecting channel frequency response data, computing the weights, and forming a null(s) in the specified direction(s). This will eliminate the long time lag associated with the current process of obtaining a data base (i.e., a set of radiation patterns as a function of frequency for each output port) and measuring the nulling performance.

Assembly of a 7-element quarter-scale array antenna using conventional crossed dipoles as elements is nearing completion. This array will replace the scale-model paraboloid antenna at the ATR for extensive testing.

C. Jammer Test Range

The quarter-scale (L-band) model of the adaptive antenna will be tested at the ATR with a separation between the adaptive antenna and jammer/user antennas of about 200 ft, rather than the 2000 ft currently being used with a single transmitting antenna. The 200-ft separation is chosen to ease the simulation of multiple jammers and is appropriate for accurate testing of the adaptive antenna. In fact, since the $R^{-1}V$ algorithm performs a least-square fit to the quiescent radiation pattern, it follows that (for a single frequency) the range dependence of the nulling antenna is identical to that of the quiescent pattern. For an earth-coverage quiescent pattern this distance is very small, but for a narrow-coverage quiescent pattern it is of the order of 200 ft. Over a band of frequencies, close-range effects modify performance. However, a computer analysis indicates that with the 200-ft separation the measured performance of a 100-MHz, 40-dB or less null within an earth-coverage angle ($\pm 9°$) is very nearly identical to performance at operational distances.

It is necessary to make use of existing turntable facilities at the ATR. This implies that the adaptive antenna be about 13 ft above the ground, while source antennas vary from 13 to 45 ft above the ground. Because of the low antenna elevations, it is necessary to use high-directivity source antennas and diffraction fences to keep ground reflections at a low level. With source antenna diameters of 5 ft (yielding an illumination taper of 0.25 dB), the ratio of the direct-ray to the reflected-ray levels in absence of diffraction fences is 12 to 14 dB for circularly polarized radiation. We hope that diffraction fences will provide an additional 16- to 18-dB increase of this ratio. Experimental tests carried out so far with three 4-ft-high fences have yielded only about a 10-dB improvement. We believe that interference of the edge-diffracted rays from each fence is limiting their effectiveness. If so, the magnitude of this effect ought to be reduced by serrating the top edge of the fences; experimental tests will be carried out to verify this hypothesis.

D. Full-Scale Antenna

Development of a lightweight UHF crossed-dipole element for possible use in a satellite array has begun. Utilizing strip-line techniques and composite materials, a single crossed-dipole (including its ground plane) is estimated to weigh less than one-half pound. Work has also begun on a lightweight balun, a quadrature hybrid, and a 4-way power divider.

E. Adaptive Nulling

The stability of the Applebaum-Howell feedback control system as a function of loop component errors is currently under investigation. We consider the values of the weights to be random processes and assess the stability of the feedback system relative to the mean values of the weights. The corresponding problem of the stability of the variance of the weight has been considered by Brennan et al.†

To date, analytical results have been obtained for a single isolated loop; numerical results for more than a single loop are currently being pursued. For the isolated loop, the stability of a first-order system (i.e., a single first-order low-pass filter in the baseband feedback section of each loop) is very insensitive to errors in the loop. Errors considered were balanced-mixer phase offset errors, inphase/quadrature (I/Q) hybrid errors, channel mismatch errors, and differential I/Q loop gain errors. Conversely, using a second-order filter (designed for maximum sensitivity to dynamic range in jammer power) leads to a stability criterion strongly dependent on loop errors. For example, a phase-offset error of 2° to 3° in the balanced mixer is sufficient to drive the loops into instability for a 40-dB dynamic range system. Techniques to compensate for this sensitivity are being studied.

F. Configuration of UHF Adaptive Array

In the past quarter, a computer program designed to evaluate the performance of a wide variety of array configurations was prepared. The physical variables which characterize the array are number, location, gain and beamwidth of the array elements, the mismatch between channels, and the length of the feeder cable to each element. The operating variables are the nulling frequency and bandwidth, the number of bits used for quantizing the element weights, and the signal frequency. The scenario variables used to test the array performance are the number, location, power, and bandwidth of the individual jamming sources.

The output from the program consists of contour diagrams of the array's directive gain, graphical presentations showing the distribution of the directive gain and of the user-to-jammer power ratio improvement over various regions in the field of view, as well as numerical data. The jammer locations and the channel mismatch parameters can be generated randomly; this allows the program automatically to examine a series of different situations and then to compile statistical data on the array performance.

In using the program, the main emphasis has been on examining the question of where to locate the elements. The conclusion is that it is better to spread the array elements nonuniformly in the plane of the array than place them in a regular fashion. This is because good resolution requires a large maximum spacing between the elements, and freedom from grating lobes within the desired field of view (±9°) requires a minimum spacing which is less than a certain upper bound. The same ratio of maximum-to-minimum spacing can be obtained using far fewer elements with a nonuniform array than with a uniform array.

For mechanical simplicity, nonuniform arrays that can be deployed with only three long booms have been surveyed. Symmetry considerations make it convenient to place the earth-coverage element at the center of the array. The simplest nonuniform array of 7 elements based on this geometry consists of the center element, the 3 elements at the ends of the booms, and 3 more placed, one on each boom, at a position along the boom. A sketch of this 7-element array is shown in Fig. 1.

---

† L. E. Brennan, E. L. Pugh, and I. S. Reed, IEEE Trans. Aerospace Electron. Systems AES-7, 254-262 (1971).

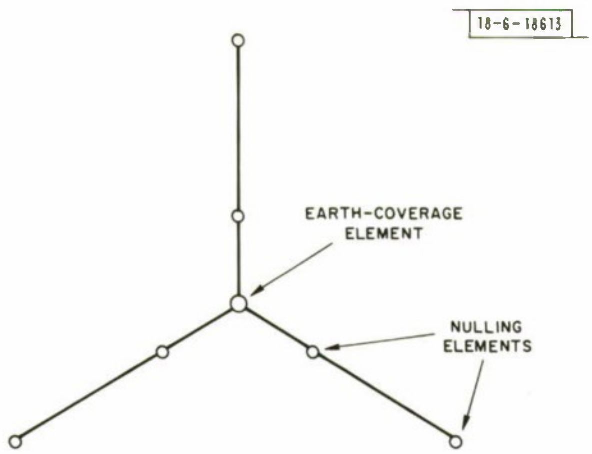

Fig. 1. 7-element double-triangle array.

The 3 mid-boom elements are placed close to the central element rather than near the outer elements to give the array the ability to perform better against multiple grouped jammers. When that situation arises, the algorithm for determining the element summing weights essentially turns off the outer 3 elements and uses the inner 4 to direct a broad null toward the jammer group.

Other investigations have shown that:

(1) The array performance is largely insensitive to the manner in which the total array gain is distributed among its elements (provided, of course, that the earth-coverage element retains enough gain for clear-mode operation).

(2) It is reasonable to consider using a 10-MHz nulling bandwidth and a 1-MHz signal bandwidth, and

(3) The feeder cables to the elements should be of equal lengths if a bandwidth of 10 MHz or greater is to be used.

Work with the program on the effects of quantization and channel mismatch is just getting under way. However, a potentially significant theoretical result on channel matching has been obtained which states that if the transfer functions of the individual nulling channels are matched across the nulling bandwidth to the transfer function of the earth-coverage channel, then the effects of the residual channel mismatch will be less damaging than if all channels are matched to some reference transfer function. In fact, the expected depth of the null on a jammer will be better by a factor $1/N$ in the former case, where N is the total number of channels.

G. Array Coupling

A simple theoretical derivation has been made of the coupling between crossed dipoles mounted on a ground plane. The resulting formula was then used to compute the coupling between co-planar arrays of crossed dipoles. In a typical design, consisting of a 4-dipole adaptive array element close to a 16-dipole transmitting element, for all three possible combinations of circular polarization (left-left, right-right, and left-right) and over the complete 300- to 400-MHz band, the coupling was found to be less than −43 dB. This result is in reasonable agreement with a similar calculation performed using an empirical formula for the inter-dipole coupling. Its implications for intermodulation interference are reassuring.

H. Bench Test Simulator

In order to test various adaptive processors, a test setup which will simulate the RF outputs of an array antenna is being designed. An analysis of the effects of amplitude and phase-tracking errors of the bench test simulator on the depth of null achievable by the nulling processor has been completed. The analysis results describe the probability of simulator errors affecting the null depth achievable by the nulling processor. For example, if the simulator amplitude errors are limited to 0.2 dB and the phase errors to 1° over the nulling band, then the nulling processor could achieve null depths on the order of 50 dB in 90 percent of the jammer simulations, if it had no amplitude and phase-tracking errors of its own. That is to say, if the bench test simulator amplitude and phase errors are limited to 0.2 dB and 1°, there is a 90-percent probability that these errors will not significantly affect the nulling capability of the processor above 50 dB null depth.

Detailed specifications for the simulator have been determined using the results of this analysis, and, from these, specifications for the individual components which make up the simulator have been derived. These specifications are being distributed to manufacturers of these components for comments and quotations of price and delivery.

RF TECHNOLOGY
GROUP 63

I. INTRODUCTION

This Quarterly Technical Summary reports on the development of receiver front ends for adaptive antenna nulling systems at UHF and at L-band. Characterization of the feedback circuitry for an analog nulling system has also been started.

Work has continued on UHF transmitter power amplifiers and IMPATT amplifiers at K-band. In addition, some considerations of X-band solid-state receivers, transmitters, and frequency sources have been addressed.

II. LES-8/9 POST-LAUNCH PERFORMANCE

A. LES-8 VCXO

The result of a 4-month temperature cycling of 4 VCXO circuits in the Laboratory has yielded no new information on the cause of the anomaly in the LES-8 VCXO. As a consequence of this fact, the long-term test was terminated.

B. K-Band Transmitters

The K-band transmitters maintained normal performance levels throughout this quarter. All associated telemetry is now reviewed at 6-week intervals.

III. RECEIVER DEVELOPMENT

A. Adaptive Nulling

Work is continuing on the development of a set of amplitude and phase-matched receiver front ends to be used in adaptive antenna nulling systems. A detailed analysis of achievable null depth vs component matching for the filters used to set system bandwidths in the direct-conversion receiver front end has been completed. These results indicate that with matching tolerances of 0.05 to 0.1 percent, null depths or interfering signal rejection will be limited to about 50 dB. This most probably represents the practical limits for front-end performance.

Design of a receiver front end for use with an L-band demonstration adaptive nulling system has been completed and is presently under construction. The design has 8 matched channels covering a frequency range of 1326 to 1763 MHz with double conversion to a final IF of 121.4 MHz. The first IF is 378.6 MHz. The front end utilizes voltage-tuned filters as RF preselectors. Purchased components are being used wherever possible, with critical components such as voltage-tuned and IF filters being designed and fabricated within the Laboratory.

Initial specifications for gains, bandwidths, and components have been generated for the IF and DC portions of the analog adaptive nuller. Components have been ordered to test various strategies in attacking some of the dynamic-range and phase-mismatch problems. Work is in progress to build zonal filters as well as wideband, minimum phase-shift clipper circuits.

B. Test Sources

During the last quarter, plans for the antenna nulling jammer source were finalized. Components and test instrumentation are in the process of procurement, and the physical layout and computer interfaces are in process of design.

Some components of the system have been built and tested, such as the comb generators and noise generators. An investigation of the feasibility of building the random-sequence generator using MECL devices is in process. Such a generator, with a higher clock rate than commercial units, could result in a much wider comb spectrum. Preliminary results look promising with an achieved clock rate of 160 MHz using fixed, hard-wired feedback taps on the shift register. The use of additional gates for selection of other feedback taps for other sequence lengths will reduce this rate.

C. X-Band Receiver

During this quarter, planning work was begun on the X-band receiver component development for the satellite applications currently under study. This has included a survey of system requirements and, from these, component specifications have been outlined to cover the possible system configurations that have been discussed. The components under development include a low-noise, high-dynamic-range preamplifier using GaAs field effect transistors (FETs), a down-converter mixer for the X-band hopped uplink, an up-converter mixer for the transmitter, and several types of interdigital filters for system development applications.

The first of the packaged GaAs FETs were recently received, and a test jig for their measurement is under construction. The transistors intended for use in the low-noise preamplifier are also being evaluated for possible use in a varactor-tuned oscillator for the receiver's first LO. Transistors from several manufacturers are being evaluated.

Work was also done on developing the basic measurement setups for the development of these components. This has included measurements of some commercial components to aid in identifying instrumentation problems.

IV. TRANSMITTER DEVELOPMENT

A. UHF Transmitter

During this report period, the slotted-section tuner mentioned in the 15 March 1977 Quarterly Technical Summary has been used to characterize a variety of UHF power transistors. The results of these measurements have been very encouraging. The tuner allows a high-power transistor to be operated over a wide range of load impedances to determine the effect of load impedance on output power and DC input power at a particular RF input power. The actual output impedance is measured dynamically by a dual-directional coupler and network analyzer which is included in the output circuit.

The load-pull measurements indicate the load impedance at the fundamental frequency for optimum gain or optimum efficiency, and indicate the gain compression and actual output power which occur at the point of optimum efficiency. Regions of instability may also be found.

Three amplifiers have been designed and constructed using load-pull measurements. One amplifier using a single 40-W device produced 41 W output with a gain of 8.9 dB and a collector efficiency of 86.4 percent at 240 MHz.

Some deficiencies exist in the tuner, and improvements are now being made. Transistor holders which have some matching circuitry are being produced so that the tuner will not be required to tune VSWRs of greater than 10:1. At VSWRs greater than 10:1, the losses in the tuner become significant and the accuracy of the measurements is impaired.

The new transistor holders will improve the accuracy of the measurements and allow devices to be measured which require very high VSWR loads in the 50- to 100-W range.

Two short-step coaxial transformer circuits were built for measuring the loss in this type circuit. These were compared with identical design microstrip circuits, and from this comparison it appears that the coaxial circuits have the potential for the lowest loss. The repeatability is also very good, but the overall size is greater than in the microstrip medium.

A number of transistors have been received and measured for basic low-frequency characteristics. Although the DC characteristics are not indicative of how the device will perform at RFs, such characterization can provide initial incoming quality control.

B. X-Band Transmitters

Solid-state alternatives to TWT power amplification at X-band have been investigated. Devices considered include FETs and bipolar transistors, with and without varactor multiplication stages. IMPATTs and IMPATT/FET hybrid configurations have also been considered. For a 10-W, 8-GHz power amplifier with approximately 40 dB gain, a configuration using state-of-the-art FETs appears promising from an efficiency standpoint, offering a power output/DC dissipation efficiency of 33 percent. If constrained to selection of commercially available devices, best efficiency (24 percent) is obtained by a 4-GHz FET amplifier followed by an X2 varactor diode.

C. K-Band Transmitter

Two more wafers with modified profiles have been evaluated, with no improvement in performance achieved over previous wafers. Additional wafers have been fabricated, one of which is presently being evaluated. No further iterations in profile modification are anticipated.

Maximum effort is presently being directed to diode packaging design and fabrication, together with final circuit optimization, for stable operation of diodes with larger areas than those used successfully to date. Two new packaging concepts which reduce package parasitics have been tried; one of these has been discontinued due to reliability problems which were encountered. Work is continuing on the other approach to eliminate mechanical alignment problems.

V. FREQUENCY SOURCES

One configuration for a stable X-band LO employs a tunable oscillator at an intermediate frequency which is phase-locked to a low-frequency standard. We have achieved phase lock between a 100-MHz VCXO and a 5-MHz standard, but have not as yet minimized phase noise near (~100 Hz) the carrier. Work is continuing in this area.

Alternate LO configurations are being investigated.

VI. AUTOMATED MEASUREMENTS

During this quarter, approval was received to upgrade the Hewlett-Packard Automatic Network Analyzer. The ANA will be shipped to Hewlett-Packard early in August 1977 for modification, and should be returned to service by early November. Methods to teach ANA users how to fully utilize the capability of the upgraded system are being developed.

SURVSAT SYSTEMS
GROUP 64

I. INTRODUCTION

Group 64 is responsible for the planning and execution of LES-8/9 experiments and transferring the associated technologies to potential operational systems. It is also involved in the Laboratory's on-going development of additional space-communications technology, and in the identification of potential applications for these developments. During this quarter, the major tasks involved the following areas:

(a) Planning, executing, and reporting on LES-8/9 communications experiments,

(b) Monitoring and controlling these spacecraft as well as initiating an upgrading of the Lincoln Experimental Satellite Operations Center (LESOC) facilities to permit more autonomous TT&C operations,

(c) Determining and maintaining accurate LES-8/9 orbit-fits,

(d) Developing General-Purpose Satellite Communications System (GPSCS) and Strategic Satellite System (SSS) spacecraft and operational configuration alternatives, and

(e) Transferring the LES-8/9 technology to the above and other potential operational systems of interest to the Department of Defense.

In addition to the efforts which are summarized below, the Group has provided support through:

(a) Participation on the communications system, terminal, and support teams involved in the System Engineering Design/Trade-off Group (SEG) efforts in support of the forthcoming GPSCS/SSS DSARC I,

(b) Furnishing extensive comments on the drafts of the final reports of the SAMSO-sponsored Survivability Analysis Group (SAG) and the Evolutionary Spacecraft Study,

(c) Helping develop the AFSATCOM II portions of the Single-Channel Transponder (SCT) Systems Specification,

(d) Reviewing two drafts of the SCT Injection System (SCTIS) Specification,

(e) Attending several Rockwell component-level Global Positioning System (GPS) SCT Preliminary Design Reviews (PDRs) as well as their system-level PDR,

(f) Participating in monthly technical reviews of General Electric's DSCS III SCT work,

(g) Assisting SAMSO and AFAL in specifying the functional goals for a forthcoming development of a modem/processor (CPM/P) for an airborne command post,

(h) Initiating internal plans to implement the DOD's intended IOC use of the wideband (500-kHz) transponder modes of LES-8/9, and

(i) Supplying information for the Aerospace Corporation's efforts to build a UHF terminal capable of receiving the LES-8/9 downlink signal.

II. LES-8/9 COMMUNICATIONS-LINK TESTING

During this quarter, the Lincoln terminals have been engaged primarily in Phase IV cooperative demonstrations and measurements with the Service terminals. The following sections summarize the activities of the Lincoln K-band command post (ABNCP) and the three Lincoln-built UHF force-element terminals in communications-link testing. Activities associated with the Lincoln K-band Navy terminal, as well as the results of cooperative jamming tests, are reported separately.

A. K-Band ABNCP Terminal

The major activities of the Laboratory's ABNCP terminal have been in four areas: support of communications-link testing by outside agencies, cooperative jamming tests, bit-error-rate measurements on the Air Force report-back link with both satellites, and various activities connected with the recording of data for orbit-fitting.

Since most Lincoln Laboratory communications experiments and demonstrations have now been completed, much of the LES-8/9 communications link testing was conducted by outside agencies this quarter. In many cases, these agencies have all the necessary resources to conduct these tests, and Lincoln participation consists only in providing command and telemetry support from LESOC. However, in a substantial number of cases, the Lincoln terminals are called on to provide communications support as well. Such tests with AFAL, Aerospace, MITRE, and ESI (a Navy contractor) have involved both the transmission of forward messages and the reception of report-back messages. No Military Utility Demonstrations were conducted this quarter; they will resume next quarter.

The Lincoln ABNCP terminal has been used extensively for quantitative bit-error-rate measurements of the Air Force report-back link. The UHF report-back uplink has been characterized by user bit-error rates vs satellite uplink receiver P_r/N_o. Instrumentation and calibration difficulties were resolved during this quarter, and the measured performance curves are shown in Fig. 2 (for LES-8, LES-9, and the Laboratory's prototype satellite – sometimes referred to as LES-8-1/2). The report-back-processor time and frequency-acquisition performance was also tested; at 28 dB-Hz P_r/N_o on the LES-9 uplink, no acquisition errors were observed in 10 min., and no false acquisitions were observed during a subsequent 10-min. period during which no signal was present (the threshold settings were unchanged between these two tests). This detection performance test was conducted with an uplink power which provided a 2.5-percent user bit-error rate (see Fig. 2). The bit-error-rate performance tests were conducted using the typical 40-character (7-bits-per-character) message format, with a new time and frequency search performed between each block of 280 user bits.

Recent experiments have explored the accuracy potential of the hardware/software complex associated with the LES-8/9 orbit-fitting process. Although the demonstrated accuracy of the orbit-fits has always exceeded what is required for communications purposes, a lull in orbit-fitting requirements and in preparations for enabling the LES-9 stationkeeping system was used to identify and isolate the degradation sources discussed below.

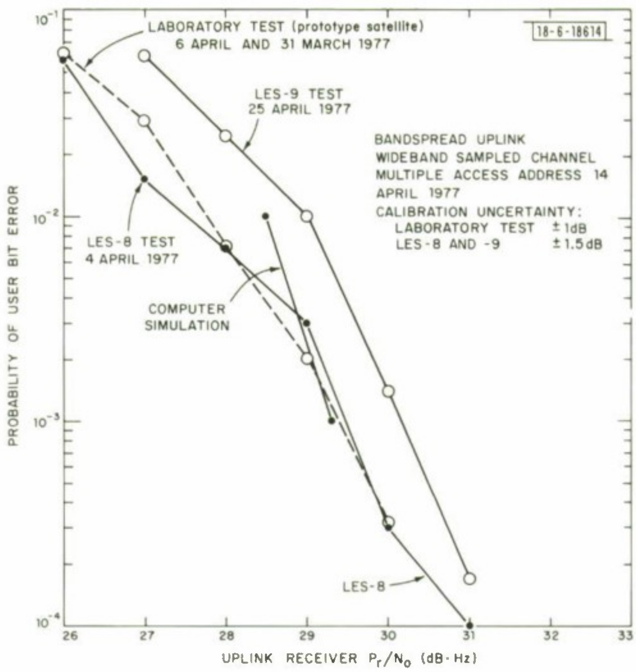

Fig. 2. UHF report-back link measured performance.

The system which measures the azimuth and elevation look-angles to the satellite from the 4-ft K-band autotrack antenna was examined and was found not to be achieving its potential accuracy. Major changes were made in the way that the optical shaft encoders in the antenna mount were interfaced to the data computer. These changes reduced the scatter in the angle measurements to the point where it is now possible to measure and compensate for small residual biases down to the resolution capability of the encoder (±0.01°).

The pseudorandom binary sequence which determines the range to the satellite was also exercised and examined for potential sources of noise in the data measurements. Changes were made in the way that the ranging system accepts this pseudorandom bit sequence from the ABNCP downlink receiver. The peak-to-peak noise on the range measurements is now within one least-significant bit in the range counter (±0.2 μsec), and there is no offset between range measurements made on the ABNCP and the Navy K-band terminals. A tabular error in the software for the predicted zero-point range to LES-9 was detected and corrected in the course of this experiment.

In the interest of obtaining higher-quality data, the interface between the coherent-Doppler measurement system and the ABNCP modem was changed in the same way as that for the ranging system. As a result of this investigation and improvement of the coherent-Doppler system, previously undetected frequency drifts in the ABNCP secondary frequency standard were exposed and corrected. This will improve the quality of the Doppler data and improve the accuracy with which the satellites' on-board frequency standards are trimmed.

Improvements in the quality of the data base used in the orbit-fitting process have made it possible to adjust the weighting of each parameter used in the prediction which, in turn, improves the accuracy and long-term drift characteristics of the process. Further, it is now

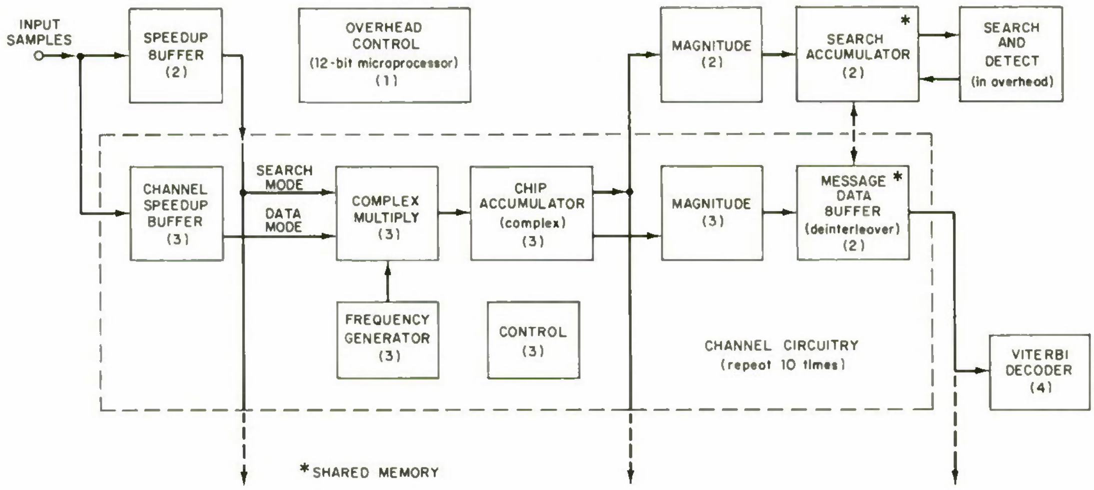

	BOARDS	ICs	POWER (W)
(1) MICROCONTROLLER	2	10	4.3
(2) COMMON ACQUISITION CIRCUITRY	10	100	27.7
(3) CHANNEL CIRCUITRY (10 channels)	14	430	22.0
(4) VITERBI DECODER	2	60	4.8
TOTAL	28	600	58.8

(a) WEIGHT 13 lb

18-6-18615

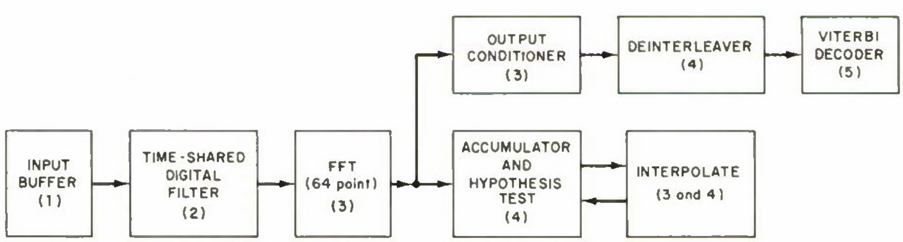

	BOARDS	ICs	POWER (W)
(1) INPUT BUFFER	2	16	3.0
(2) TIME-SHARED DIGITAL FILTER	4	112	9.9
(3) FFT (including microcontroller)	5	48	11.0
(4) ACCUMULATOR (main memory)	15	129	36.7
(5) VITERBI DECODER	2	60	5.0
TOTAL	28	365	65.6

(b) WEIGHT 13 lb

18-6-18616

Fig. 3. Report-back-processor configurations and weight, power, and space estimates. (a) Design "A," and (b) design "B."

possible to use the programs to detect inconsistencies (biases) between the different parameters. The subject of a continuing investigation is the appearance of an apparent small residual bias in the zero-point delay for LES-9. (The maximum expected drift in the orbital predictions resulting from this bias would be approximately 0.01°/day in mean anomaly.)

B. UHF Force-Element Terminals

The Lincoln UHF force-element terminals (FETs) have been used to monitor forward-link messages during various inter-agency tests in this quarter. FET-1 (the laboratory prototype) provided low-data-rate telemetry as needed. FET-2 was used to support the bit-error-rate measurements of the UHF report-back link which were reported above. FET-3 remains installed in AFAL's C-135 aircraft No. 12662 awaiting further flight testing.

UHF multitone jamming experiments were conducted using FET-2 and the laboratory prototype satellite. These experiments uncovered a problem in the terminal which necessitates minor modification and a repeat of the experiments.

III. SIOP PROCESSOR SPACE, POWER, AND WEIGHT ESTIMATES

Some of the spacecraft configuration alternatives under study for possible GPSCS/SSS applications include a dedicated SIOP processor onboard the system's satellites. This processor typically includes a 10-channel forward link/CINCNET demodulator and decoder, and a 10-channel force-element report-back demodulator and decoder. All the links are assumed to operate at a user rate of 75 bps and to use LES-8/9 modulation and coding. The primary processing burden derives from the time and frequency acquisition and correction required of the report-back processor (since the associated force-element terminals are not required to do more than coarse precorrections on uplink transmissions).

Members of Groups 64, 67, and 69 have jointly prepared estimates of the weight and power needs of a spacecraft SIOP processor. Since the estimates are dependent on the acquisition algorithm used in the force-element report-back link, certain issues were first addressed analytically to insure that the candidate designs provided adequate detection, estimation, anti-jam and false-alarm properties. Two acquisition criteria were established for a signal in white Gaussian noise. At the selected acquisition threshold [about 1.5 dB below the threshold signal-to-noise (S/N) ratio for communications], the first criterion requires that the correct time-and-frequency-offset hypothesis be chosen with probability $\geqslant 0.9995$. The second criterion requires that, with the threshold set for a false-alarm rate of 1 per day, the detection threshold be exceeded by the correct-hypothesis test statistic with probability $\geqslant 0.9995$. The first criterion was also applied in the presence of a partial-band multitone jammer.

Existing (non-spaceborne) report-back-processor designs were reviewed, and two candidate configurations [see Figs. 3(a) and (b)] were defined which satisfy the criteria. They differ primarily in the acquisition algorithm used to exploit the existing preamble structure transmitted by the force element. Design "A" uses twenty-six 10-msec "chips" spread uniformly over the 2-sec preamble to test the time-and-frequency hypotheses; design "B" uses 60 "chips" from half the preamble (i.e., 1 sec) for the same purpose (allowing the hypotheses to be tested in two groups). The size, power, and weight estimates shown in the figures assume the exclusive use of bipolar TTL technology.

The associated forward and conferencing-link processor discussed above requires 2 logic boards, and would add 4.5 W and 0.5 lb to the report-back-processor totals shown in Figs. 3(a) and (b).

COMMUNICATIONS SYSTEMS
GROUP 67

Group 67 has responsibility for architecture concept development for future MILSATCOM systems and for analytical investigation of spacecraft signal processing techniques. In separate tasks, the Group is providing support to the ongoing MILSATCOM architecture efforts at both SAMSO and the MILSATCOM System Office (MSO) of the Defense Communications Agency (DCA). The Group is also involved in analytic studies and simulation of onboard signal processing techniques that could be useful in next-generation MILSATCOM systems, particularly those operating in the UHF band that serve a large number of small, mobile terminals.

I. MODULATION DESIGN

A. Introduction

Some satellite communication applications require close packing of users when no coherent phase reference is available at the receiver. To accomplish the above, a phase-comparison version of sinusoidal frequency-shift keying (PCSFSK)† has been proposed. The performance of PCSFSK in the presence of Gaussian white noise and crosstalk due to adjacent closely packed users is considered. Analyses of the effects of noise and crosstalk are presented, and the results of simulations for such systems are described.

B. Signal Description

The received PCSFSK signal is

$$x(t) = \sum_{n \text{ even}} \sqrt{2E_b}\, b_n\, s(t - nT) \cos(2\pi f_o t + \Theta)$$

$$+ \sum_{n \text{ odd}} \sqrt{2E_b}\, b_n\, s(t - nT) \sin(2\pi f_o t + \Theta) \qquad (1)$$

where

E_b = signal energy per channel bit,

T = time per channel bit,

f_o = carrier frequency,

Θ = random phase angle,

b_n = +1 or −1,

---

† B. E. White, I. Kalet, and H. M. Heggestad, "Offset Quadrature Phase-Comparison Modulation Schemes for Low-Crosstalk Communication," presented at IEEE Intl. Conf. on Communications, Chicago, June 1977.

and

$$s(t) = \frac{1}{\sqrt{T}} \cos\left(\frac{\pi}{2}\,\frac{t}{T} - \frac{1}{4}\sin 2\pi\,\frac{t}{T}\right) \quad . \tag{2}$$

In complex notation, the signal may be described as

$$x(t) = \mathrm{Re}\{\underset{\sim}{x}(t)\} \tag{3a}$$

where

$$\underset{\sim}{x}(t) = \sqrt{2E_b}\;\underset{\sim}{v}(t)\; e^{-j(2\pi f_o t + \Theta)} \tag{3b}$$

and

$$\underset{\sim}{v}(t) = \sum_{n\ \mathrm{even}} b_n\, s(t - nT) + j \sum_{n\ \mathrm{odd}} b_n\, s(t - nT) \quad . \tag{3c}$$

Figure 4 depicts $\underset{\sim}{v}(t)$, the complex envelope of $\underset{\sim}{x}(t)$. In each 2T channel symbol interval on either the in-phase or quadrature channel, the signal phase is either 0° or 180° (except for the unknown phase offset Θ) depending on the sign of the appropriate b_n factor. Figure 4 shows the b_n's located at those portions of $\underset{\sim}{v}(t)$ which they affect. Information is transmitted by defining a 2T channel symbol, e.g., the in-phase channel symbol affected by b_o, as a reference symbol. Then, a determination is made on whether $b_1 = b_0$ or $b_1 \neq b_0$, to yield the first bit of information. The next bit is determined by whether $b_2 = b_1$ or $b_2 \neq b_1$, and so on. With proper coding and interpretation, this system may be designed to be insensitive to an integral number of shifts in bit timing.

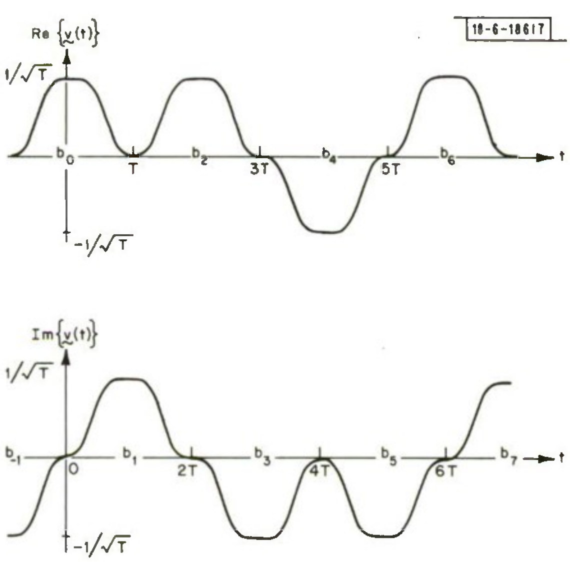

Fig. 4. Complex envelope, $\underset{\sim}{v}(t)$.

C. Receiver Description

Figure 5 shows the receiver structure of a PCSFSK receiver. The output of the receiver is a complex number AB*. For determining whether $b_1 = b_0$ or $b_1 \neq b_0$, the factor A is derived by filtering the signal over the [−T, T] interval, and B* is derived by filtering the signal

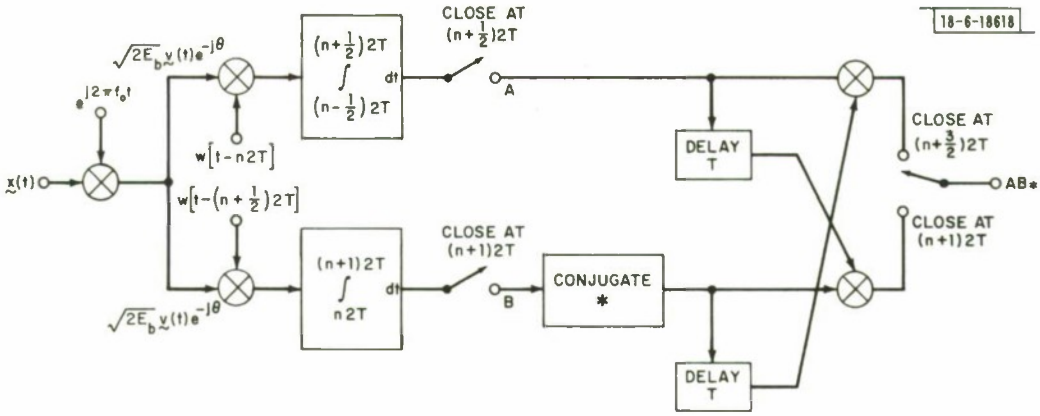

Fig. 5. Receiver for PCSFSK.

over the [0, 2T] interval. The filter window w(t) equals s(t) for a matched filter receiver, the receiver whose performance is analyzed here.

Figure 6 portrays the complex decision space, and the points at which AB* may lie in the absence of noise. If $b_1 = b_0$, AB* falls on one of the points labeled ①, ②, or ③. If $b_1 \neq b_0$, AB* falls on one of the points labeled ④, ⑤, or ⑥. (In Fig. 6, $\rho = 0.194$ is the cross-correlation between s(t) and s(t + T) for SFSK. Exactly where AB* falls depends on b_{-1} and b_2, as well as b_0 and whether $b_1 = b_0$ or $b_1 \neq b_0$. An examination of Fig. 6 indicates that a reasonable rule for determining whether $b_1 = b_0$ or $b_1 \neq b_0$ is whether $\text{Re}\{AB*\} > 0$ or $\text{Re}\{AB*\} < 0$, and this rule is the one used in the performance calculations.

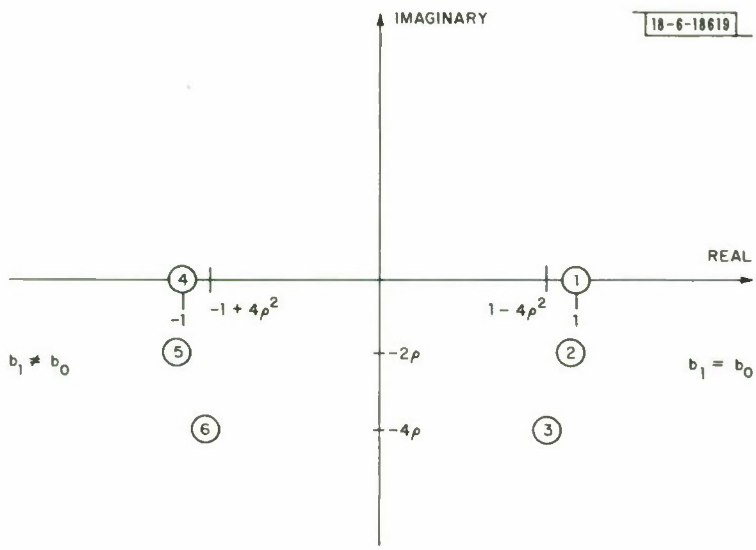

Fig. 6. PCSFSK decision space.

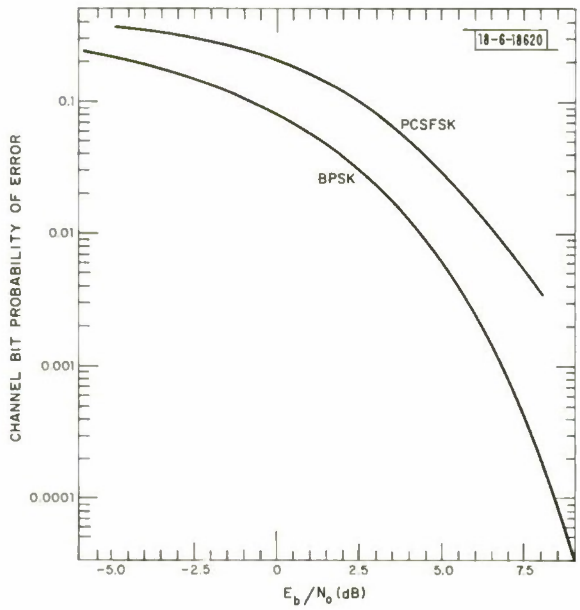

Fig. 7. Bit probability of error performance for PCSFSK.

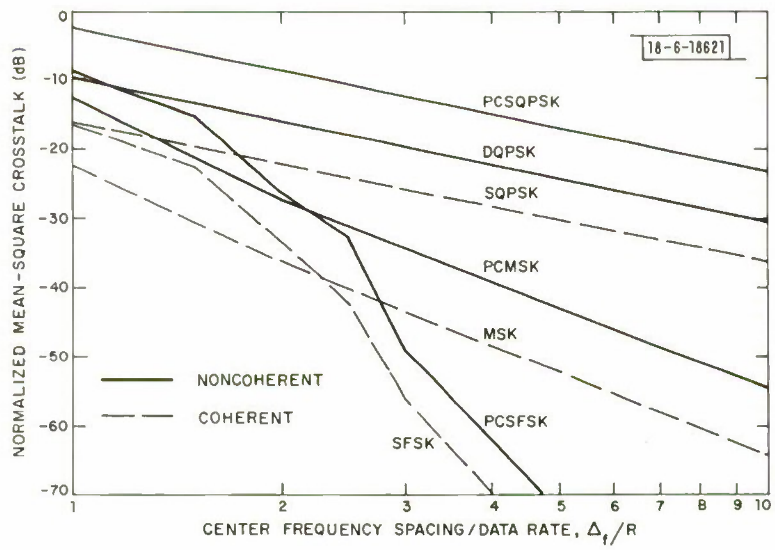

Fig. 8. Crosstalk performance as a function of Δ_f/R.

D. Performance Against White Noise†

The PCSFSK receiver of Fig. 5 has been simulated in the presence of white Gaussian noise. Figure 7 shows the performance characteristics found. The probability of error for any particular phase-comparison ($b_{n-1} - b_n$ transition) decision is graphed against E_b/N_o, the channel bit energy-to-noise power density ratio. Figure 7 also compares the PCSFSK receiver performance with that of the optimal receiver for binary antipodal signaling (BPSK), indicating a degradation of only about 2.5 dB for the same level of error probability – a performance nearly equal to DQPSK.

E. Crosstalk Results

Mean Square Crosstalk‡ is a measure of the amount of interference caused by an adjacent user signal separated by Δ_f Hz from the desired user signal (both signal data rates being the same). By considering crosstalk curves for different techniques, we can compare the close packing performance of these methods.

Figure 8 shows the normalized (with respect to minimum distance between signals) crosstalk curves plotted as a function of Δ_f/R for a number of coherent and phase-comparison techniques including MSK,§ PCMSK, SQPSK,‡ PCSQPSK, SFSK,¶ PCSFSK, and DQPSK.

The curves show that for Δ_f/R greater than about 2.2, SFSK and PCSFSK have the best crosstalk performance for coherent and phase-comparison methods, respectively. The crosstalk curve for PCSFSK drops dramatically for a larger value of Δ_f/R, implying that signals at a large frequency separation will have little impact on crosstalk even if these signals are much stronger than the desired user.

F. PCSFSK Simulation

A PCSFSK demodulator has been simulated. The received signal considered consisted of white noise plus the desired SFSK user and a large number (7) of similar SFSK (equal-data-rate) interfering users, with each user separated by Δ_f Hz from adjacent users. The interfering users were all 20 dB greater than the desired signal. (This approximates the worst possible case in the communication channels under study.) The interfering users were assumed to have random bit timings and phase angles with respect to the desired signal.

The simulation results for two cases of interest are shown in Fig. 9. The dashed curve represents the bit probability of error as a function of Δ_f/R for the case in which no noise is present, and the solid curve represents the case in which $E_b/N_o = 7$ dB for the desired user (27 dB for each interfering user). From these curves we see that we could space signals at a distance of $\Delta_f/R = 2.2$ without suffering any appreciable loss in performance.

---

† L. S. Metzger, "Performance of Phase Comparison Sinusoidal Frequency Shift Keying," submitted to IEEE Trans. Commun.

‡ I. Kalet, "A Look at Crosstalk in Quadrature-Carrier Modulation Systems," to be published in IEEE Trans. Commun., September 1977.

§ M. K. Simon, IEEE Trans. Commun. COM-24, 845-856 (1976).

¶ F. Amoroso, IEEE Trans. Commun. COM-24, 381-384 (1976).

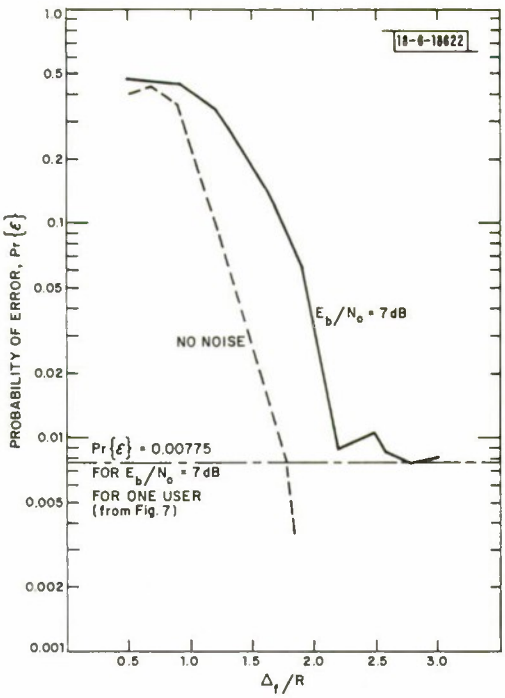

Fig. 9. Simulation results. Probability of error vs Δ_f/R for PCSFSK. Desired user plus one interfering user (20 dB > desired user, R = 4.8 kbps).

II. DEMAND ASSIGNMENT

Investigations are being made on methods of assigning satellite circuits to users on demand in a processing satellite using FDMA uplinks and TDM downlinks. In a fully shared demand assignment (DA) scheme, users would access the satellite controller via an uplink request channel and would be assigned downlink slots from the pool of all available downlink slots. In a partitioned DA scheme, each class of user is assigned a downlink slot from within a smaller pool of downlink slots. When an insufficient number of downlink slots are available, a user's request is either blocked and cleared (blocked calls cleared, BCC) or blocked and queued (blocked calls queued, BCQ) for subsequent servicing.

The request channel would be one of the satellite's FDMA uplinks. It would be organized into a frame of K slots, each of which will accommodate the request sequence plus a 40-msec guard time to account for the uncertainty in the user's location. The users would acquire slot timing from the downlink and make requests at random in one of the request slots. The number of request slots and request channels can be easily adjusted to accommodate varying rates of requests.

For Poisson distributed request arrivals at an average rate of 1 arrival/frame, the probability of a user's request being successfully received is 0.88 for 5 request slots/frame, 0.97 for 15 slots/frame, and 0.99 for 15 slots/frame with 3 uplink request channels. In all cases, the mean waiting time before a request is successfully received is less than one frame. A 64-bit request at 2400 bps would result in 15 slots (request and guard time) in a 1-sec frame. Thus, calls arriving at an average of one per second can successfully request access to the satellite with high probability in less than 1 sec.

Once a request for service is successfully received, it must be routed to the allocation algorithm that assigns an uplink FDMA channel and a downlink TDM slot for the circuit connection. Since the request arrivals and the holding times are random, some overhead must be paid in the number of circuits required to service a given mean traffic intensity. The grade-of-service is measured by the probability a call is blocked (because a circuit is not available).

The number of circuits required to satisfy a given traffic intensity in a fully shared DA system with BCC is shown in Table I for blocking probabilities P_b = 1, 5, and 10 percent. The utilization ρ is a measure of the average fractional usage of the available circuits, and therefore indicates the efficiency with which the satellite resources are being allocated. Note from Table I that a lower grade-of-service and a larger pool of traffic provide a more efficient utilization of the satellite resources.

The total circuits required can be decreased by allowing some number of requests to be queued rather than cleared when no circuits are available. Table II shows the percentage decrease as a function of traffic load for a queue length of 25. Queueing gains are largest for low total traffic loads.

TABLE I

CIRCUITS REQUIRED AND CIRCUIT UTILIZATION FOR VARIOUS TRAFFIC INTENSITIES IN A FULLY SHARED DEMAND ASSIGNMENT SYSTEM WITH BLOCKED CALLS CLEARED

Traffic Load (Erlangs)	Number of Circuits Required			Utilization ρ		
	$P_b = 0.01$	$P_b = 0.05$	$P_b = 0.10$	$P_b = 0.01$	$P_b = 0.05$	$P_b = 0.10$
1	5	4	3	0.20	0.24	0.30
10	18	15	13	0.50	0.63	0.69
100	117	105	97	0.85	0.90	0.93
1000	1029	966	909	0.96	0.98	0.99

TABLE II

PERCENTAGE OF CHANGES IN REQUIRED CIRCUITS DUE TO QUEUEING REQUESTS AND PARTITIONING USERS ($P_b = 0.01$)

Total Traffic Load (Erlangs)	Decrease in Required Circuits Due to Queue of 25 Requests (percent)	Increase in Required Circuits Due to Partitioning Users into 10 Equal Classes (percent)
1	60	–
10	39	78
100	10	54
1000	2	14

On the other hand, a sizable increase in the number of circuits required results from partitioning the users and satellite resources into several smaller pools. This is also shown in Table II for the case of 10 equal-user classes. Note that a severe penalty is incurred for not fully sharing the satellite resources, unless each of the smaller pools represents substantial traffic itself.

Since military SATCOM is organized into separate user nets and since these user classes are not all identical, additional work is required to determine the form and effects of practical partitioning. Preliminary results indicate the same trends as noted above for the case of identical user classes. Work will continue in this area to verify these results and indicate efficient schemes for allocating the satellite resources in the real military operational environment.

SPACECRAFT TECHNOLOGY
GROUP 68

I. INTRODUCTION

This report period saw the start of a serious effort to define a command/control scheme suitable for use in an advanced technology satellite, such as GPSCS. The Attitude Control System (ACS) study was virtually completed. A new effort was started to evaluate the Electrostatically Suspended Gyro (ESG), which appears to be a promising answer to the gyro reliability and lifetime problems for communications satellites. A novel design for a magnetic bearing suspension system for momentum or energy storage wheels was completed, and parts for a demonstration unit are being machined. The development of a new automated facility for testing the radiation hardness of LSI electronics components is proceeding; integration of most of the major hardware items is completed.

II. COMMAND TELEMETRY

A. Satellite Support

There was no Command Telemetry support required by Group 68 for LES-6 or LES-8/9 during this quarter.

B. 16-Bit Analog/Digital (A/D) Converter

A printed-circuit board has been laid out and fabricated for the analog portion of the 16-bit A/D converter that has been under development for several months. The preliminary wirewrap version exhibited excessive noise pickup, which the new board is designed to reduce. The new configuration should be ready shortly for testing.

C. Automated Test System

During the past quarter, work has proceeded on a stand-alone automated test facility, as discussed in the 15 March 1977 Quarterly Technical Summary. Specifications for a small computer to control the system were sent out for quotations, and the quotes were evaluated. The selected vendor is Digital Equipment Corporation, who proposed a modified DECLAB 11/03 system and quoted delivery at 150 days ARO.

A circuit to implement a standardized interface to the IEEE instrument bus has been designed. This circuit represents the major portion of in-house design effort that will be necessary for the automated test system. It fits on a single plug-in card and implements virtually all IEEE specified functions for a talker or listener. In addition, several other options have been provided to increase its general usefulness. Other users of the IEEE bus can take advantage of this card after construction and testing of the prototype is complete. Efforts are under way to interface this card to a digital-data generator, controller, and a serial time code receiver for use in the test system.

D. Telemetry/Command System Studies

A review of technical articles and information on the design and content of various command and telemetry systems has been started. This effort is expected to continue over the next few months, culminating in a proposed control scheme for a satellite consisting of a common bus supporting a communications payload which incorporates adaptive routing and adaptive nulling antennas.

E. Microprocessors

A project to evaluate a specific commercial microprocessor has begun. Of immediate interest is an I^2L device that has prospects of becoming flight-qualified. Our immediate goal is to become familiar with the electrical and functional aspects of the chip, and to lend support to the radiation tests to be performed on it. Over a longer term, the instruction set, computational power, and architectural characteristics will be evaluated. A basic, one-board processing kit for this microprocessor has been ordered.

III. CONTROL SYSTEMS

A. LES-8/9 Support

A complete investigation of LES-8 TGG drift-rate change reported last quarter showed that the problem was not related to switching of converter loads, but was due to a switchover from TOC B to TOC A shortly before the converter switch. The 100-kHz system clock for the TGG is fed from the TOCs, and when the switch occurred the TGG logic was interrupted, causing the TGG wheel float to move 9.7 μin. axially and the state of magnetization of the spin motor to change. These, in turn, caused a slight change in average power drawn by the TGG, hence the shift in drift-rate bias.

A procedure for detecting possible erroneous thruster firings was incorporated into the LESOC automatic alarm system.

A program was developed to analyze the momentum wheel average power vs wheel speed and temperature. It was used to determine that there has been no change in power consumption over the first year in orbit, which indicates that the bearings are not degrading.

B. Attitude Control System (ACS) Studies

The study of an ACS for a candidate GPSCS satellite is complete except for a final decision on the stabilization system to be used when coasting during the Backup Mode. The linearized computer model of the Backup Mode is now operating and proving very useful. We expect to finalize this proposal during the next quarter.

As mentioned in the last Quarterly Technical Summary, the backup system will bypass gyros and derive yaw error by on-board processing of the sun elevation angle. In-house tests, using a LES-8/9 backup SAZ sensor and a 5-kW solar simulator, indicate that yaw errors can be measured with present sensors to an accuracy of $\pm 0.01°$ over a minimum of 200 orbital azimuthal degrees.

C. Attitude Sensor Studies

The main effort of the last few months has been to investigate the present development status of the ESG and to determine its applicability to a synchronous orbit ACS. Besides the study of available documents and reports, a visit was made to manufacturers of two different types of ESG. Present information indicates that the ESG should be a prime candidate for yaw axis control on future satellites, even though none have been flown in space to date. The main deterrent to the use of standard gyros on communications satellites is their limited and unpredictable lifetime. The ESG, in contrast to standard gyros, has a very simple geometry with no apparent wearout mechanisms. Its drift performance, while not as good as a standard gyro, easily meets the requirements for satellite attitude control. Work will continue in the next quarter to determine the areas of the ESG that should be modified or improved to meet the requirements of satellite application.

D. Pulsed Plasma Thrusters (PPTs)

During the last quarter, we successfully completed a long-term vacuum test of three flight PPTs. The logic circuits in these thrusters had been modified to protect input ICs against voltage spikes. During this report period, the seven remaining thrusters were likewise modified and all but two have been tested; these two will be tested within three weeks. All ten thrusters will then be stored as flight-qualified units for possible future use.

IV. POWER

A. LES-8/9 Support

Sufficient information has been gathered over the past year to allow close comparison of RTG predicted behavior and measured results. Bimonthly testing, data reduction, and trend evaluation will continue with Group 68 support. Long-term communications asset utilization and contingency plans are being fomulated by the Air Force supported principally by Group 64, but with assistance in satellite power and system operations planning by Group 68.

B. Flywheel Energy Storage

System trade-off studies of flywheel vs other forms of energy and angular momentum storage for spacecraft applications have been performed. For energy storage, flywheels are more attractive than NiCd batteries on a watt-hour-per-pound basis, but not much better than predicted NiH_2 battery performance. The use of the flywheel technologies of high-strength, low weight rotors and magnetic bearings looks very attractive for attitude control momentum wheels. A test magnetic bearing of novel design, suitable either for momentum wheel or energy wheel applications, is now being fabricated. Electronics for the suspension have been built, and permanent magnet parts ordered. Most items have been machined. Assembly and testing will extend through the next quarter. A subcontractor has begun design work for a motor-generator that is compatible with the magnetic bearing design.

C. Terrestrial Solar Photovoltaic Power

Group 68 continues to support this program at a level of one full-time staff member with one technician. An additional staff engineer is being provided for consultation. His critical design review of the Nebraska solar-powered irrigation project has revealed a few possibilities for design improvement, but no fundamental technical problems. Assistance with control and component performance trade-off analysis will continue into the next quarter.

D. Batteries

A nickel-hydrogen battery has been purchased and should be received for in-house testing and evaluation during the next quarter.

V. DEVICE PHYSICS

A. Radiation Hardening Technology

During this quarter, our continuing effort to assess the state-of-the-art in LSI device radiation hardening focused primarily on nuclear transient radiation effects. Much information was obtained by visiting other facilities and gathering pertinent documents. We are in the process of evaluating this information to assess the impact of nuclear hardening on future satellite design.

We received further confirmation this report period of the hardness of some current I^2L technology – specifically that of a particular commercial microprocessor. Since there are several attractive features to this device, we have initiated an evaluation effort aimed eventually at testing its suitability for spacecraft use in a radiation environment.

B. Radiation Test Facility

Test facility efforts this quarter have concentrated on optimizing system integration techniques. The overall interface design for analog stimulus/response measurements has been finalized, and should be constructed next quarter. A flexible patch-card approach will be used which should permit rapid adaptation of the facility to a variety of measurement configurations.

A general-purpose interface box, providing 15 channels of 8-bit D/A control, was designed and tested this quarter, with assembly of remaining cards under way. The interface box will be used primarily to program a commercial pulse generator for system use. Software to control the interface box has been written and debugged, while software specifically adapted to pulse generator control will be written next quarter.

Detailed design began this quarter for the overall system-controlled digital stimulus/response package required for testing microprocessors and memory systems at high speeds in a radiation environment.

C. Radiation Exposure Tests

No radiation tests were conducted this quarter, but the test facility did support the Group 83 solar-cell characterization effort. This relatively simple test determined diode I-V characteristics over 8 decades of current in under 2 sec. It gave us a chance to exercise a fully integrated test setup involving stimulus/response control, rapid data acquisition, data reduction, printing, plotting, and the software development necessary to implement these functions. This test also provided reassuring affirmation of the value of a general-purpose automated test facility.

VI. SPACECRAFT CONFIGURATION STUDY

The in-house study of various candidate GPSCS satellite configurations continued during this quarter. Also, staff support has been provided to SAMSO in preparing for a DSARC I review of the GPSCS program. The focus of the present in-house study is on a 7-element, lightweight, UHF nulling antenna with both analog and digital versions of the adaptive nulling circuits sized for comparison. The satellite uses six identical, but separate, UHF TDM downlinks. A preliminary design of this version of the spacecraft will be completed during the next quarter.

SPACECRAFT COMMUNICATIONS PROCESSORS
GROUP 69

I. ADAPTIVE ANTENNA NULLING

A. Introduction

Lincoln Laboratory continues to approach the adaptive antenna nulling problem from two different directions – a primarily digital block-processing scheme and an analog feedback scheme. Most of the work in Group 69 has been directed toward realization of an experimental all-digital system.

B. Experimental Block Processing Hardware

1. A/D Converters

Further work is continuing in the area of an A/D performance measurement setup. A static test card has been designed and is in the electronic shop awaiting layout.

A specification has been written for 10- and 12-bit, 10^6 conversion/sec converters, and an RFI is being sent out. Further investigation of vendor capability in the area will be undertaken.

The detailed design of a subranging scheme using two 8-bit converters in cascade and having effective throughput of 10^6 12-bit conversions/sec has been completed and the printed-circuit card has been fabricated. All components for this card have not yet been received.

2. Signal Filter

Of the various filters which might be used to suppress user signals when computing the interference correlation matrix, the "accordion filter" has been investigated in the most detail. This filter has equally spaced narrow stop bands, one for each user, and passes all other frequencies. The stop-band spacing is changed randomly at every frequency hop. This requires that the hopping pattern of each user be very slightly different from that of the other users.

An alternative signal filter concept which does not impose this requirement on users has randomly spaced stop bands, but the stop-band spacing does not change from hop to hop. Unfortunately, implementations of such filters are not competitive in size, weight, and power with the accordion filter, which has a simple implementation.

3. Correlator

The correlator computes the interference correlation matrix R for the (complex) signals from the 8 data channels (receiving antennas). R is estimated using sparse and random data samples; for the demonstration system, about 200 randomly sampled data sets are used out of the 13.3×10^3 data sets available over a typical dwell period of 13.3 msec.

Since R is Hermitian ($r_{ij} = r^*_{ji}$), only the upper triangular and diagonal elements need be computed. These 36 complex numbers are computed using a 1-chip parallel 12- × 12-bit multiplier, an adder, and memory. Detailed design and parts procurement for the correlator are now in progress.

4. Data Buffer

Responses to the RFI for the buffer memory have been received and evaluated. A purchase order has been prepared and is awaiting approval.

Error-correction logic has been designed based on a Hamming code for single-error correction and double-error detection. This will be done over eight 24-bit channels. A test card has been designed which will enable testing of the error-correction logic using an Intel 8080 microcomputer. Wirewrap lists are currently being written for the above cards. A memory exerciser which tests the buffer memory with and without error-correction logic is now in the initial design stage.

5. Central Processor Unit

The specification of a 16-bit minicomputer to be used as the nulling processor in the demonstration block-processing system was written and sent to five computer vendors.

Preliminary design of the input and output interfaces for the demonstration system nulling processor has been completed, execution speed of the $R^{-1}V$ algorithm has been studied, and coding of the computation of contents of the combiner memory, given $R^{-1}V$, has also been completed.

6. Data Combiner

The pseudomultiplication scheme to be implemented in the signal combiner was outlined in the last Quarterly Technical Summary (15 March 1977). The detailed design of this subsystem is now in progress.

7. Group Converter

Both analog and digital versions of the group converter were studied, including power estimates. So far, the best digital scheme takes about twice as much power as an analog design. The search for more efficient digital algorithms continues.

C. Lookahead Scheme

An alternative scheme being investigated has been called "lookahead." One set of channels is operated in the same way as in the block-processing scheme previously described. Meanwhile, a similar set of channels with a different frequency synthesizer looks ahead in frequency bands to which the system soon will hop. During the looks ahead, the interference correlation matrices for these frequencies are estimated, which is easy to do because the users' signals are not present to confuse the estimation. In order to avoid problems of precision matching being required between lookahead and nulling channels, it is possible to interchange their roles such that each set of channels does its own looking ahead. The lookahead scheme involves extra synthesizers, downconverters and A/D converters, but it does away with the need for a signal filter and for a data buffer memory. A major system advantage of the present block-processing approach is its resistance to nonstationary jamming strategies. The lookahead scheme may be vulnerable to such strategies and must be further explored in this light.

D. Alternative Formulation of Block-Processing Approach

Mathematically, if the statistics of the jammers are characterized by a correlation matrix R, the ideal weight vector is given by $R^{-1}V$, where V is a given steering vector. In practice, the correlation matrix is not known but must be estimated from observations. It is possible, however, to find the optimum weights, given the steering vector and the raw observations, without necessarily computing the correlation matrix itself. Such a formulation has been worked out; it gives exactly the same weights as the $R^{-1}V$ formulation, as one might expect, but the computations called for by the new method, while more numerous, require less precision than is required by the earlier approach. Specific and detailed comparisons of the two approaches will be carried out.

E. Precision Tolerances and Dynamic Ranges

1. Processor Word Lengths

Estimates of the word-length requirements for a digital nulling processor were reported in the previous quarter. Those estimates have since been verified by computer simulation.

2. A/D-Converter Characteristics

Limitations of dynamic range and sampling-time jitter have been investigated for A/D converters. The dynamic range of an A/D converter is the maximum S/N ratio (SNR) that can be delivered at the device output:

$$\text{dynamic range} = \max(\text{SNR}) = \max\left(\frac{\text{input signal power}}{\text{converter quantization noise}}\right) \quad .$$

The dynamic range, evaluated for Gaussian input signals, is indicated in the table below:

Converter Bits	Dynamic Range (dB)
8	40
10	51
12	62

Timing jitter may be modeled as a noise-inducing phenomenon, the effect of which is to reduce the achievable null depth of the nulling system. This effect has been quantified as follows:

$$\text{mean square timing jitter} \leqslant \frac{1}{W}\sqrt{24 \cdot \text{null depth}}$$

where W is the nulling bandwidth. For example, a null depth of 50 dB requires that timing jitter be less than 150 nsec for a 1-MHz nulling bandwidth.

3. System Issues

Estimations of the dynamic range requirements at key system points have been made. These requirements apply to any nulling system, analog or digital. A digital system has, additionally, a precision requirement for the A/D converters; this requirement has also been estimated. The key system points are the inputs to the nulling system and the demodulator inputs (nulling system output).

At the input to the nulling system the total dynamic range is determined by an upper constraint, the maximum jammer power which can be nulled sufficiently to permit communication, and by a lower constraint, the system thermal noise. However, if an AGC is used, a smaller dynamic range (minimum dynamic range) can be presented to any A/D converter in the system. This minimum dynamic range is determined taking note of the fact that, with strong jamming, the jamming (rather than the thermal noise) limits the communications capability and the user signals (at a rate of 75 bps) will have margin over the system thermal noise. This margin can be relaxed to zero in determining the minimum dynamic range. Total dynamic range at the

TABLE III

DYNAMIC RANGES†

Maximum Array Processing Gain (dB)	At Nulling System Input: Total Dynamic Range (dB)	At Nulling System Input: Minimum Dynamic Range (dB)	A/D (bits)	AGC Range (dB)	At Demodulator Input: Total Dynamic Range (dB)
30	88	37	8 (min) 10 12	47 36 25	67
40	98	47	10 (min) 12	47 36	67

† For the following conditions: N = 8 elements, maximum array gain = 23 dB, users receive earth-coverage gain (17 dB), system noise figure = 7 dB, terminal EIRP = 30 dBW.

demodulator inputs is determined by communication requirements and system bandwidth. Table III gives dynamic range requirements and A/D precision requirements for two assumed values of processing gain (signal-to-jammer differential gain) and for several choices of A/D precision.

The total dynamic range at the element ports exceeds the range of any A/D converter that is likely to be available in the near future; an AGC is therefore required, as shown. The minimum dynamic range A/D (so indicated) is chosen to match the minimum dynamic range requirement. The advantage in choosing an A/D with a greater-than-minimum dynamic range is the reduction of AGC range and a reduction in the precision or tracking requirement of the AGC.

F. Analog Feedback Scheme

Most of the work on the analog adaptive nulling system is reported by Group 61. Group 69 is helping with the digital control unit for the analog feedback version of the adaptive antenna nulling array which is currently in the preliminary design phase. Current effort is focused on system definition, system interface requirements, and system component specifications.

Functionally the digital controller will perform as a mini-CPU and as a storage device for use in control and monitoring of the analog adaptive feedback loops. Storage will be provided for both quiescent beam-steering vectors and for dynamic sampled values of the antenna element weight-control voltages. The latter information will be used for loop initialization during frequency hopping. In addition, the controller will be configured in such a manner as to allow for bidirectional information transfer during system testing, and will incorporate the necessary control capability to allow various modifications of the adaptive algorithms to be implemented and tested (variable threshold hard limiters, slew rate control, dynamic range control, etc.). The controller will be designed to operate in conjunction with the test bed hardware, and will receive clocking and frequency-hopping information from it. This information will then be used to control the operational sequencing of the adaptive analog feedback loops (initialization interval, adaption interval, weight "freeze" for pattern measurement, etc.).

We expect that, during the coming quarter, the digital control unit will become more completely specified, both functionally and in terms of actual operational parameters, and preliminary demonstration hardware will be designed, built, and tested.

II. COMMUNICATIONS PROCESSOR

A. Group Demodulators

Detailed design and simulation studies have both proceeded during this quarter, and a realistic design of a group demodulator for phase-comparison sinusoidal frequency shift keying is now quite well understood.

A realistic simulation reflects the proposed hardware design in the simplified block diagram of Fig. 10(a). In particular, the input consists of I and Q samples of the sum of users' signals and white Gaussian noise of variable intensity. The input is scaled according to total power and quantized to 8 bits. Clipping limits the magnitude of each sample to be less than unity. A complex multiplication by 8-bit coefficients, each less than unity, results in a product which is truncated and accumulated in 12-bit real and imaginary accumulators. Bit decisions using phase-comparison detection are made on 7-bit truncations of the accumulated data. The final 1-bit decision is then stored until read out by the communications output processor (COP). Figure 10(b) shows the hardware implementation in greater detail, with indications of the associated quantization.

Thus far, the simulation has aided in our choice of quantization to achieve a receiver having performance within 1/2 dB of an unquantized receiver with one user at 4800 bps at various noise levels, and nearly identical in performance to an unquantized receiver in terms of minimum frequency spacing between two users with 20-dB relative power differences. The simulation confirms that truncating the 12-bit accumulator output to 7 bits before passing the output to the decision region retains acceptable error-rate performance. The program allows study of the complex interactions and effects of number of users, data rate, and noise on bit error rate.

A complete 2-channel A/D converter, including the sample and holds, suitable for use in a group demodulator has been constructed. In addition, a test simulator for group demodulator testing has been built and tested. This unit has one synthesizer and one modulator, and can therefore simulate one uplink user. A unit which can simulate 16 users is now being designed.

B. Microprogrammed Adaptive Routing Controller

The circuit boards necessary for initial turn-on of the MARC (microprogrammed adaptive routing controller) have been designed and fabricated. The backplane for the MARC is being fabricated. Some of the microcode test routines and instructions have been coded. A program to transfer files from the IBM-370 to the NOVA 3/12 development system is being debugged, as is the DIMARC interface between the NOVA and the MARC.

The COP is being redesigned to provide for multiple downlinks. The design of a single COP with several outputs (downlinks) was investigated. This design was found to impose too many constraints on the data rates and frame rates at the downlinks. A second design which uses multiple COPs with less capability was investigated. This design makes the separate downlinks completely independent of one another.

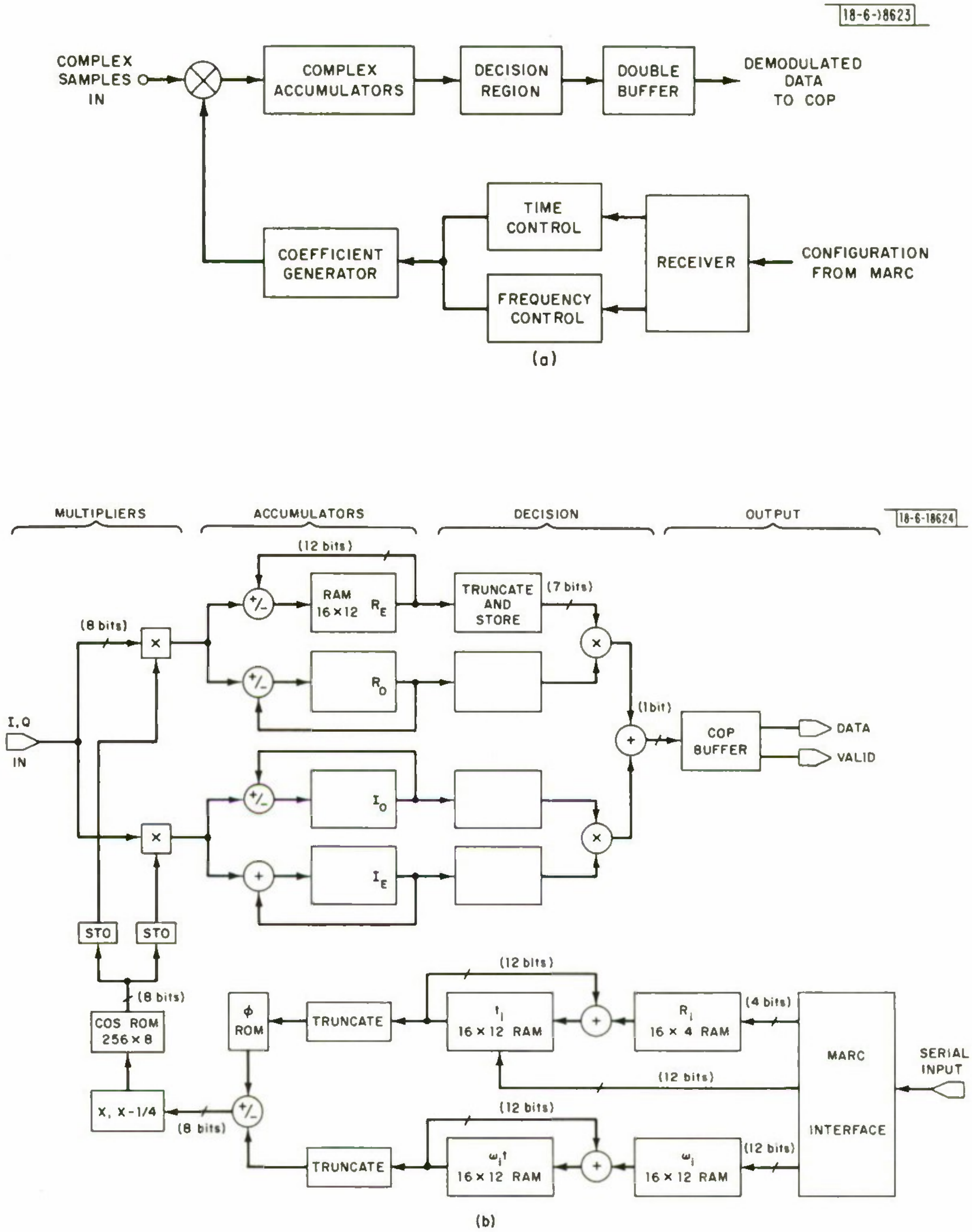

Fig. 10. Group demodulator – (a) simplified diagram; (b) detailed diagram.

MECHANICAL ENGINEERING
GROUP 71

I. TECHNOLOGY PROGRAM

A. Electromechanical Deployment Devices

Design of a servocontrolled spacecraft antenna boom deployment mechanism has been completed. Essentially, the mechanism is a powered hinge device consisting of a brushless DC torque motor whose output torque is amplified by an "Orbidrive" speed-reducer unit. Boom deployment will be controlled in velocity by pulse counting, and in position with a resolver. The closed-loop performance of these powered hinges will control acceleration forces on the boom, provide telemetry data on boom position, and deploy booms in any desired programmed sequence of deployment including intermittent positioning. Its reversible feature, which enables recycling on command, will facilitate all necessary ground-systems testing of a deployable array.

A 12 oz.-in. DC brushless torque motor using electronic commutation has been selected. The output torque will be conditioned to the desired speed and torque by the Orbidrive speed reducer. This will allow a 90° boom deployment within 1 min.

The basic design has been modularized to the extent that two of these units can be combined into a single redundant drive. Redundancy applies to the motors, pivot bearings, and Orbidrive unit. The weight of the redundant unit is approximately 1.5 lb. Specifications and component control drawings are being prepared for vendor selection and fabrication of a development model.

B. Mechanical Subsystems – Energy Storage Wheel

A development model Energy Storage Wheel has been designed and released for fabrication. The elements of the energy wheel system are magnetic bearings, rotor, motor generator, position sensors, auxiliary touch-down bearings, and support structure. The magnetic-bearing design consists of a radially passive and axially active system. The primary purpose of the prototype unit is to develop and test the magnetic bearings. For this reason, the optimum system design has not been pursued with respect to high-speed operation, rotor design, and dynamic considerations.

Assembly and testing of the development model unit will start during the next quarter.

C. Analyses

Dynamic and static analyses have been conducted to determine the feasibility of using advanced composite materials to fabricate lightweight, high-strength-and-stiffness antennas.

TRW's LMP computer program, which was developed to determine the mechanical properties of multiple-layer composites, has been included in the time-sharing system at Lincoln Laboratory.

Utilizing STRUDL dynamics and plotting capability, together with the LMP program and the Tektronix scope, real-time analyses have been conducted for various antenna configurations. The results to date indicate that composites theoretically show great promise as antenna structural components. The next phase is to determine if structures, made principally out of composite materials, can be fabricated and assembled.

D. Materials and Processes – Vacuum Outgassing Material

During the LES-8/9 satellite development era, polymeric materials were constantly being evaluated for their contamination effect, specifically their influence on non-volatile-residues (NVR). NASA has provided a document, "A Compilation of Outgassing Data for Spacecraft Materials" (TND-7362), which lists the percentage total weight loss (%TWL) and percentage volatile condensable material (%VCM). Briefly, this NASA technique heats a sample for 24 hr in vacuum at 125°C, and collects on a cooled disk (25°C) the outgassing products a few centimeters away.

Our technique augments the NASA data by measuring the %TWL at three temperatures, 25°C, 60°C, and 100°C for periods of 24 hr each. This enables us to determine whether the material, if properly pre-vacuum baked for a period of time and at a specified temperature, can be made clean and usable.

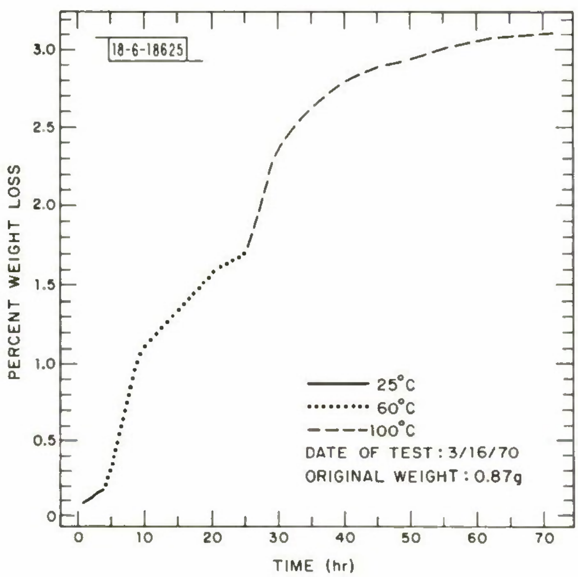

Fig. 11. Vacuum outgassing of a silicone resin.

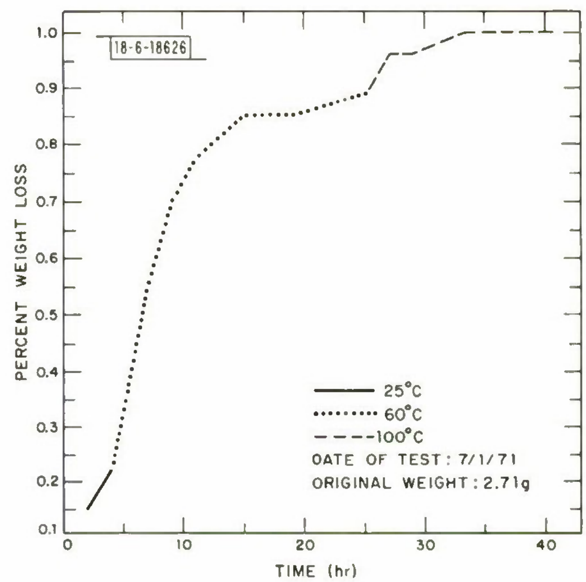

Fig. 12. Vacuum outgassing of a graphite epoxy laminate.

We are currently transposing data from chart strips to computer output form to make the information more readily available. Two typical readouts are shown in Figs. 11 and 12. One is a low-outgassing epoxy graphite laminate, and the other a high-outgassing RTV (room-temperature vulcanizer) silicone.

E. Electronic and RF Support

1. Packaging Low-Power Schottky Logic

A design study is currently under way to evaluate various techniques that could be used in packaging low-power Schottky logic on multilayer boards. The study is based on utilizing the same size board as in LES-8/9; however, the power dissipated will increase from 0.5 to 2.5 W per board. A design has been released to fabrication for a prototype unit that will be used for further evaluation. The significant features in the new design are:

(a) Increase in copper in multilayer construction (i.e., 4 oz. copper for Vcc and Gnd layers),

(b) One-piece mounting frame with center web,

(c) Increase in size of heat sink on enclosure walls.

A comparison weight study between the LES-8/9 logic boxes and the proposed design indicates that the incorporation of the above features will result in a weight increase of approximately 40 percent per box.

2. Computer-Aided Harness Interconnections System

A computer-aided harness interconnections system has been developed and is ready for implementation in the design of future spacecraft harnesses. Some of the advantages over the method used in the past are:

(a) Elimination of handwritten wiring sheets,

(b) The edit capability of changing one end termination while the computer automatically changes the other end,

(c) The capability of generating printouts by function (i.e., all 26-V lines, TLM points, commands, etc.),

(d) Printouts sorted by wire number, unit number, functions, etc.,

(e) Capability to obtain up-to-date wire listings at any console,

(f) Capability to print out an entire string of an individual function.

We are presently working on a program that will determine the length of each wire. This information would be useful in determining line losses, harness weight, etc.

3. Diode Mounting Test Fixture

A diode mounting test fixture has been designed and fabricated and will be used in conjunction with a capacitance bridge to characterize varactors used in voltage-tuned filters for the adaptive nulling UHF receiver front end.

F. Antenna Development

To date, four antenna configurations have been developed. They consist of a 4-dipole receive array (54 × 54 in.), a 16-dipole low-power transmit dipole array (130 × 130 in.), an 18-element dipole receive array, and a deployable helix antenna.

The first two have been analyzed dynamically utilizing computer programs, and appear satisfactory in the launch environment. The latter two configurations are being developed as of this writing.

A report has been received from TRW which predicts the physical properties of the Hercules Graphite Epoxy Composite Material (HMS-3501-6) which we anticipate using as the basic antenna structural material. These data will provide a "yardstick" with which to compare the properties measured in an in-house test program.

We predict a weight for the 4-dipole receive array, minus RF components, of 1.64 lb. This weight includes the back structure plus 4 ft of support boom. The predicted weight of the 16-element low-power transmit array is 18.7 lb, again minus RF components but including back structure.

G. Solar Torques

Radiation torques were predicted for a spacecraft of the following configuration:

Body	Tetragonal with an 80- × 80-in. forward platform and 80- × 72-in. side panels.
Solar panels	Two panels, each having 108 ft^2 area with a pressure point 22.167 ft from central axis; booms are 6-in.-diameter.
Antenna	Major torque-producing surfaces are twelve 2-in.-diameter booms with a projected area of 44.6 ft^2.

Force calculations were based on NASA Report SP-8027, where

$$F = \frac{IA}{C} \{-[(1 + Crs) \cos\theta + \frac{2}{3} Crd] n + (1 - Crs) \sin\theta\ S\} \cos\theta \quad .$$

The solar constant $I = 1.353\ kW/m^2$, and Crs and Crd are coefficients of specular and diffuse reflection, respectively. The solar panels were assumed to be 2 ft forward of the C.G. location. Calculations were also made with the C. G. being collinear with the solar-panel axis. All torque values were figured for spacecraft in the ecliptic and equatorial planes. The resulting maximum per-orbit torques in μlb-ft are presented below for comparison.

	Solstice	Ecliptic
Solar panel 2 ft forward of C. G.	40.2	47.9
Solar panel on C. G.	1.4	1.5

It will be noted that the solar-panel position has a large effect on the solar torques.

H. Antenna Test Models

1. Phase I Array (Modified Quarter-Scale)

A 14-element test array consisting of six radial booms attached to a center hub, with a rectangular ground-plane and two dipole elements with a hybrid network mounted at the outer end of each boom and at the center hub, has been designed for mounting on a positioner. A tubular steel model tower has been designed to support the positioner and test array while the latter is positioned over the center of rotation of an azimuth rotary table. Fabrication and installation are complete, and testing will start during the next quarter.

2. Phase II Array

The configuration of an intermediate quarter-scale array has not been finalized, but the design of a support structure capable of adapting to a multiplicity of arrays is being completed. A center ring and mounting flange will accept two, three, four, six, or twelve equally spaced radial booms on which various types and sizes of ground planes and dipoles (elements) may be interchanged or rearranged. This development work is scheduled for next quarter, while the Phase I temporary array is being tested at the Antenna Test Range.

L. ATS-F' Residual Assets

A request from Air Force Systems Command (AFSC) has been made to ESD to place an indefinite hold on all ATS-F' systems and support equipment, including the Thermal Structural Model and Earth Viewing Modules, until SAMSO/YAT has completed its task of assessing all other potential space test program (STP) missions which could use all or part of the subject assets.

ELECTROMECHANICAL SYSTEMS ENGINEERING
GROUP 73

I. COMPUTER SOFTWARE DEVELOPMENT

A. STRUPLOT

STRUPLOT, a new ICES subsystem for interactive plotting of STRUDL data and results, is now being used in production. Initial response to its versatility indicates a very successful subsystem. The plotting of stress and/or strain contours has also been added to the system and appears to be working well.

The planar finite elements developed for electromagnetic field problems have been tested and seem to work successfully. Consistent edge loadings are now able to be computed internally, while consistent surface loadings and body loadings are being developed for these elements.

B. LLTTA

Modifications to the Lincoln Laboratory Transient Terminal Analyzer (LLTTA), to provide louver subroutines, have been completed and checked. Final documentation in the form of a users' manual is being prepared.

The thermal implications of proposed logic devices were investigated during this period. Power levels from 0.08 to 1.0 W for low-power Schottky devices are being considered. Parametric curves showing logic board temperature rise as a function of uniformly distributed power dissipation and the amount of copper in the voltage and ground distribution network were presented during working group meetings. The requirements for providing local heat sinks for devices dissipating as much as 1 W were emphasized, and design alternatives were discussed.

Since most devices will have a dissipation level of 0.08 W, a realistic design was established for a 4- × 5-in. board typical of those used on LES-8/9 based on an upper limit of 2.4 W total per board. The goal was to control the maximum temperature rise of the device located at the center of a board close to that found for the LES-8/9 design. Changes include the following:

(1) Two 4-oz. copper layers for board construction, rather than 1-oz. layers for LES-8/9.

(2) Efficient use of a one-piece board mounting frame to aid in heat distribution to the box side walls.

(3) Providing mounting to the box side wall from the center of the mounting frame rather than the top.

(4) Increasing the box side wall from the mounting frame attachment to the baseplate from 1/16 to 1/4 in.

(5) Bonding devices to the board to reduce the interface thermal resistance.

Table IV below shows the results of a detailed analysis on the new design compared with the results found for LES-8/9. Although total power dissipation per board is greater by a factor of five and device dissipation greater by a factor of eight, maximum device temperatures are similar. The results of a weight study (discussed in the Group 71 section) indicate that total box weight increase for the new design is approximately 40 percent more than for LES-8/9 logic systems.

TABLE IV

THERMAL CHARACTERISTICS OF LOGIC PACKAGES

Maximum Board Temperature Rise for Uniformly Distributed Power Dissipation

Board	Power Dissipation per Board (W)	$R^{1}_{Board-Box}$ (°C/W)	$R^{2}_{Box-Base}$ (°C/W)	R_{1+2} (°C/W)	ΔT_1 (°C) Board-Base	Total Temperature Rise $\Delta T_1 + \Delta T_2$ (°C)
LES-8/9	0.44	24	$12.9\ (\frac{1}{2} \times \frac{1}{16} \times 4)$	36.9	16.2	19.0 (LES-8/9)
New Design	2.4	5	$2.4\ (\frac{1}{2} \times \frac{1}{4} \times 3)$	7.4	17.8	21.0 (New Design)

Temperature Rise, Device to Board

Device	Device at Board Power Dissipation (W)	$R^{1}_{Junction-Case}$ (°C/W)	$R^{2}_{Case-Board}$ (°C/W)	R_{1+2} (°C/W)	ΔT_2 (°C) Junction-Board
LES-8/9, SN54L95 Flat Pack, No Bonding	0.01	76.0	200	276	2.8
New Design, L.P. Schottky Bonded to Board	0.08	10.0	30.0	40	3.2

GLOSSARY

ABNCP	Airborne Command Post
ACS	Attitude Control System
A/D	Analog to Digital
AFAL	Air Force Avionics Laboratory
AFSATCOM	Air Force Satellite Communications
AFSC	Air Force Systems Command
AGC	Automatic Gain Control
ANA	Automatic Network Analyzer
ATR	Antenna Test Range
BPSK	Binary Phase-Shift Keying
COP	Communications Output Processor
CPU	Central Processor Unit
DA	Demand Assignment
D/A	Digital to Analog
DCA	Defense Communications Agency
DIMARC	Debugging Interface for the MARC
DSARC	Defense System Acquisition Review Council
DSCS	Defense Satellite Communications System
EIRP	Effective Irradiated Power
ESD	Electronic Systems Division
ESG	Electrostatically Suspended Gyro
FDMA	Frequency-Division Multiple Access
FET	Field Effect Transistor
FET	Force-Element Terminal
FFT	Fast Fourier Transform
GPS	Global Positioning System
GPSCS	General-Purpose Satellite Communications System
IC	Integrated Circuit
IF	Intermediate Frequency
IMPATT	Impact Ionization Avalanche Transit Time
IOC	Interim Operational Capability
LES	Lincoln Experimental Satellite
LESOC	Lincoln Experimental Satellite Operations Center
LLTTA	Lincoln Laboratory Transient Terminal Analyzer
LO	Local Oscillator
LSI	Large-Scale Integration

MARC	Microprogrammed Adaptive Routing Controller
MECL	Motorola Emitter-Coupled Logic
MILSATCOM	Military Satellite Communications
MSK	Minimum Shift Keying
MSO	MILSATCOM System Office
NASA	National Aeronautics and Space Administration
NVR	Non-Volatile Residues
PCSFSK	Phase-Comparison Sinusoidal Frequency-Shift Keying
PDR	Preliminary Design Review
PPT	Pulsed Plasma Thruster
RF	Radio Frequency
RTG	Radioisotope Thermoelectric Generator
SAG	Survivability Analysis Group
SAMSO	Space and Missile Systems Organization
SAZ	Solar Array Sensor
SCT	Single-Channel Transponder
SCTIS	SCT Injection System
SEG	System Engineering Design/Trade-off Group
SIOP	Single Integrated Operations Plan
S/N	Signal to Noise
SSS	Strategic Satellite System
STP	Space Test Program
STRUDL	Structural Design Language
TDM	Time-Division Multiplex
TGG	Third-Generation Gyro
TOC	Telemetry Output Converter
TTC	Tracking Telemetry and Command
TTL	Transistor-Transistor Logic
TWT	Traveling-Wave Tube
UHF	Ultra-High Frequency
VCXO	Voltage-Controlled Crystal Oscillator
VSWR	Voltage Standing-Wave Ratio

UNCLASSIFIED

SECURITY CLASSIFICATION OF THIS PAGE *(When Data Entered)*

REPORT DOCUMENTATION PAGE

READ INSTRUCTIONS BEFORE COMPLETING FORM

1. REPORT NUMBER ESD-TR-77-122	2. GOVT ACCESSION NO.	3. RECIPIENT'S CATALOG NUMBER
4. TITLE *(and Subtitle)* Space Communications		5. TYPE OF REPORT & PERIOD COVERED Quarterly Technical Summary 1 March – 31 May 1977
		6. PERFORMING ORG. REPORT NUMBER
7. AUTHOR*(s)* Barney Reiffen and Charles W. Niessen		8. CONTRACT OR GRANT NUMBER*(s)* F19628-76-C-0002
9. PERFORMING ORGANIZATION NAME AND ADDRESS Lincoln Laboratory, M.I.T. P.O. Box 73 Lexington, MA 02173		10. PROGRAM ELEMENT, PROJECT, TASK AREA & WORK UNIT NUMBERS Program Element Nos. 65705F and 63431F Project Nos. 649L and 2029
11. CONTROLLING OFFICE NAME AND ADDRESS Air Force Systems Command, USAF Andrews AFB Washington, DC 20331		12. REPORT DATE 15 June 1977
		13. NUMBER OF PAGES 56
14. MONITORING AGENCY NAME & ADDRESS *(if different from Controlling Office)* Electronic Systems Division Hanscom AFB Bedford, MA 01731		15. SECURITY CLASS. *(of this report)* Unclassified
		15a. DECLASSIFICATION DOWNGRADING SCHEDULE

16. DISTRIBUTION STATEMENT *(of this Report)*

Approved for Public Release

~~Distribution limited to U.S. Government agencies only; test and evaluation; 18 August 1977. Other requests for this document must be referred to ESD/TML (Lincoln Laboratory), Hanscom AFB, MA 01731.~~

Distribution Unlimited

17. DISTRIBUTION STATEMENT *(of the abstract entered in Block 20, if different from Report)*

18. SUPPLEMENTARY NOTES

None

19. KEY WORDS *(Continue on reverse side if necessary and identify by block number)*

satellite communications	digital processing	LES-6
optical communications	K-band	LES-8
antennas	LES-5	LES-9

20. ABSTRACT *(Continue on reverse side if necessary and identify by block number)*

This Space Communications – Division 6 Quarterly Technical Summary covers the period 1 March through 31 May 1977. It includes satellite communications work performed within Divisions 6 and 7. Other work in Division 6 is reported separately.

DD FORM 1473 1 JAN 73 EDITION OF 1 NOV 65 IS OBSOLETE

UNCLASSIFIED

SECURITY CLASSIFICATION OF THIS PAGE *(When Data Entered)*

☆U.S. GOVERNMENT PRINTING OFFICE: 1977—A0883/123

DEPARTMENT OF THE AIR FORCE
AIR FORCE GEOPHYSICS LABORATORY (AFSC)
HANSCOM AIR FORCE BASE, MASSACHUSETTS 01731

REPLY TO ATTN OF: SULR (Diane Corazzini, 4553) 2 May 1985

SUBJECT: Approval of Reports to be Downgraded to "Statement A"

TO: AFGL/SULL
Research Library

1. The following reports have been approved by the Public Affairs Office (ESD/PAM) for downgrading to Statement A:

ESD-TR-77-270	ERASE: An Overview
ESD-TR-77-30	Theory and Operating Characteristics of TRAPATT Amplifiers
ESD-TR-77-69	Space Communications
ESD-TR-77-122	Space Communications
ESD-TR-77-229	Space Communications

2. ESD-TR-77-348 "LES-8/9 Antenna Systems. Vol 2: S-Band Telemetry" has been approved on the condition that a reference be removed. Attached is page iii, with the reference deleted, enabling this report to now be labelled "Statement A."

Diane Corazzini
DIANE CORAZZINI
Research Publications

1 Atch
Corrected page for ESD-TR-77-348